COLLISION AVOIDANCE FOR RECTILINEAR ENCOUNTERS BETWEEN SPHERICAL SPACE OBJECTS VIA THE SCENARIO APPROACH

Romain Serra[(1)], **Denis Arzelier**[(2)], **and Aude Rondepierre**[(3)]

[(1)]*CNRS, LAAS, INSA, Univ de Toulouse, 7 avenue du Colonel Roche F-31400 Toulouse, France, +33 5 61 33 63 27, serra@laas.fr*

[(2)]*CNRS, LAAS, Univ de Toulouse, 7 avenue du Colonel Roche F-31400 Toulouse, France, +33 5 61 33 64 76, arzelier@laas.fr*

[(3)]*IMT, INSA, Univ de Toulouse, 135 avenue de Rangueil F-31077 Toulouse, France, +33 5 61 55 93 17, aude.rondepierre@math.univ-toulouse.fr*

Abstract:

This paper addresses the problem of active collision avoidance for an operational satellite with an orbital debris. The thrusting strategy is designed as a single velocity increment performed at a time fixed in advance. Due to uncertainty affecting the position and velocity of the two objects, its computation can be cast into a chance-constrained optimization problem. Here, the model of rectilinear encounters between spherical objects enables to tackle it via the so-called scenario approach. In the scenario program, constraints and their gradients with respect to the control vector are computed analytically thanks to the f and g functions, assuming Keplerian dynamics to propagate the effects of the maneuver. Two test cases including a real collision alert illustrate the performance of the proposed method.

1. INTRODUCTION

The ever-growing population of space debris has become a constant threat for Earth satellites. On-ground tracking radars allow to foresee potential collisions and consequent alerts are sent to operators several days before a would-be conjunction of a debris with one of the spacecraft they monitor. These messages describe the geometry as well as position and velocity at some reference time of a pair of potentially colliding objects. Because of the uncertain nature of the data, the risk is computed via a probabilistic metric. When the collision probability is too high compared to the safety threshold, the operator would then need to perform an evasive maneuver. The design of such an operation is driven by fuel-consumption in order to have the slightest impact on mission lifetime. Assuming that statistical information is available for characterizing uncertainty, an intuitive formulation of the problem belongs to the class of chance-constrained optimization problems where at least one constraint is probabilistic [15], [12], [4].

Since chance-constrained problems are generally hard to solve, simplifying assumptions are usually made to reduce the dimension of the optimization space or even to avoid the probabilistic formulation. In [11], the optimization process is decoupled: the direction is optimized at first before minimizing the magnitude independently. In the context of formation flying, the method described in [16] does not directly handle the collision probability. Instead, the velocity increment is designed to achieve a fixed distance of closest approach between the two mean trajectories. A similar approach is used in [14], where execution time and thrust direction are heuristically fixed *a priori* so that the collision

avoidance maneuver is only optimized in magnitude. On the other hand, in [10], uncertainty is tackled via robust optimization and convex relaxations rather than via a chance constrained optimization problem formulation. In the present paper, no relaxation is done concerning the optimization variables and the probabilistic formulation is dealt with indirectly.

This study focuses on the design of a single maneuver to be executed at a fixed time before conjunction. Assuming high-thrust chemical propulsion, an impulsive idealization of the finite powered control is considered. In practice, this kind of space operation is usually effective enough to reduce the risk to an acceptable level. The conjunction is assumed to be a rectilinear encounter involving spherical objects [2, 7]. As in [11], the effects of the maneuver are computed assuming Keplerian dynamics. Consequently, orbit propagation may be done analytically thanks to the Lagrange coefficients f and g [3, 8, 9]. The original chance-constrained problem is handled via the so-called scenario approach [5, 6]. Using this method, admissible solutions of the genuine probabilistic optimization problem are provided with some predefined confidence level when a convexity property of the realizable set is verified [6]. Unfortunately, this is not the case for the problem of collision avoidance tackled in this paper. Still, scenario approaches offer a practical and useful way to the user for designing effective fuel-efficient maneuvers. This is demonstrated by the results obtained with the numerical examples. The first one, originating from a real case collision alert, validates the proposed approach by comparison with a heuristic method while the second one, simulating an encounter on an elliptical orbit, shows its efficiency.

2. ENCOUNTER MODEL

In a possible collision between a pair of Earth-orbiting objects, the active actuated satellite is referred to as the primary object denoted by the subscript p, while the space debris, assumed to be passive (non actuated) is called the secondary object denoted by the subscript s.

A typical alert provides the operator with an uncertain estimate of both objects' position $\mathbf{r}$ and velocity $\mathbf{v}$ at some reference time $t = 0$, chosen when the mean trajectories are close to each other. The system of coordinates can be any Earth-centered frame, such as the Geocentric Equatorial Coordinate System [17]. Using the notations previously introduced and superscripts for time evaluation, the uncertain parameter is $\mathbf{q} = (\hat{\mathbf{r}}_p^0, \hat{\mathbf{v}}_p^0, \mathbf{r}_s^0, \mathbf{v}_s^0)$, lying in a domain of uncertainty $\mathscr{Q} \subseteq \mathbb{R}^3 \times \mathbb{R}^3 \times \mathbb{R}^3 \times \mathbb{R}^3$. The hat stands for the fact that $\hat{\mathbf{r}}_p^0$ and $\hat{\mathbf{v}}_p^0$ describe the primary state if no maneuver is performed. When uncertainty is modeled via probability distributions, the states of the two objects are usually modeled with independent multivariate normal laws [7]. However, in the present approach, no assumption on the probabilistic nature of the random vectors is needed. The only requirement is to be able to trial the general random vector $\mathbf{q}$ that describes uncertainty.

A specific model - namely short-term encounters [2] - has been developed to describe conjunctions with high relative speed at stake. Such a case typically occurs in low-Earth orbit where orbital velocities are the highest in magnitude. The short-term model is based on one main approximation: the relative motion between the two objects is considered as a uniformly rectilinear trajectory. Also, in this model, uncertainty on velocities is usually neglected, but this assumption is not required by our approach and will not be requested here.

The last assumption is that each object is geometrically modeled with a sphere. In this context, the collision set i.e. the set of initial ($t = 0$) relative coordinates leading to a collision on an infinite time horizon is an infinite right cylinder of revolution, referred to as the tube of collision [7]. Let us briefly explain why. First of all, one needs to introduce the so-called combined object [7]. Defined for any time t, it is the set of relative coordinates between the primary and secondary centers such that the two objects are intersecting. Because of the spherical assumption, the combined object is in fact independent of time and is also a sphere, whose radius R equals the sum of the objects' radii (see Figure 1). Under the uniform rectilinear assumption of the motion, the collision set is the translation of the combined object centered at the origin over an infinite time horizon along the direction given by the relative velocity. As a result, the tube of collision is an infinite right cylinder of revolution, whose axis contains the origin and is directed along the relative velocity.

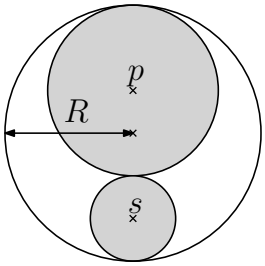

Figure 1: Combined sphere of the two objects

3. CHANCE-CONSTRAINED FORMULATION FOR THE PROBLEM OF COLLISION AVOIDANCE

Basically, the goal of an avoidance maneuver is to minimize fuel-consumption while ensuring that the probability of collision over time remains sufficiently small according to mission requirements. Assuming high-thrust propulsion, a maneuver is modeled as an instantaneous jump in the velocity of the primary object, referred to as an impulse. The date of the burn $\tau \leq 0$ is fixed in advance and is not part of the optimization process. Its choice can be based on heuristic considerations or on operational constraints such as visibility windows. As a result, the control vector reduces to a single velocity increment $\Delta\mathbf{v}$. Usually, there is only a need for a very slight velocity correction to avoid collision. For this reason, the control set $\mathscr{X} \subset \mathbb{R}^3$ is chosen as some ball centered at zero with a relatively small radius. Assuming a single steerable thruster, fuel-consumption equals the Euclidean norm of the velocity increment $\|\Delta\mathbf{v}\|$ [13, Chapter 6]. In order to obtain a differentiable function, the performance index is chosen as $\|\Delta\mathbf{v}\|^2$.

In our model, for a given occurrence of the uncertain parameter $\mathbf{q}$, the condition for a collision to occur can be written - as will be shown later - as a single inequality $c(\Delta\mathbf{v}, \mathbf{q}) < 0$, where $c : \mathscr{X} \times \mathscr{Q} \mapsto \mathbb{R}$. Therefore, the chance-constrained problem writes as:

$$\min_{\Delta\mathbf{v} \in \mathscr{X}} \|\Delta\mathbf{v}\|^2 \quad \text{s.t.} \quad \mathbb{P}\{c(\Delta\mathbf{v}, \mathbf{q}) < 0\} \leq \varepsilon, \tag{1}$$

where the maximum risk $\varepsilon \in (0, 1)$ is defined by the user.

For a given $(\Delta\mathbf{v}, \mathbf{q})$, the computation of c is done in two steps. First, the effect of $\Delta\mathbf{v}$ can be computed by propagating the initial state $(\hat{\mathbf{r}}_p^0, \hat{\mathbf{v}}_p^0)$ backwards in time to its date of execution τ, adding the

velocity increment and propagating forwards to the reference time. Then, the objects' states are plugged in the equation defining the tube of collision. All the details are given in Section 5..

Despite the quadratic cost function and its convexity property, Problem (1) is hard to solve if only for the computation of the chance constraint itself. Therefore, it is tackled indirectly with a scenario approach described below.

4. A SCENARIO APPROACH

The scenario approach can provide admissible solutions to a chance-constrained problem [5]. Instead of dealing with a probabilistic constraint, it aims at solving a min-max problem on a large but finite number of occurrences of the uncertain parameter. In the present case, as the cost function does not depend on the random vector, the resulting problem described hereafter is a deterministic minimization problem.

4.1. The Scenario Program

The scenario approach aims at solving a so-called scenario program [5]. First of all, one needs to sample N vectors $\mathbf{q}^{(1)},\dots,\mathbf{q}^{(N)}$ in $\mathscr{Q}$. The scenario program associated to (1) then writes as:

$$\min_{\Delta\mathbf{v}\in\mathscr{X}} \|\Delta\mathbf{v}\|^2 \quad \text{s.t.} \quad c(\Delta\mathbf{v},\mathbf{q}^{(i)}) \geq 0 \quad \forall i = 1,\dots,N. \tag{2}$$

Note here that the cost function appearing in the scenario program (2), is unchanged but the chance constraint has been replaced by a finite number of deterministic conditions, easier to evaluate. In general, local solutions of such a problem can be obtained by use of state-of-the-art optimization solvers, especially if the gradient of c with respect to the control vector can be computed analytically.

4.2. Solutions of the Scenario Program

Let us first define the feasibility set $\mathscr{K}_\mathbf{q}$, for $\mathbf{q}$ in $\mathscr{Q}$:

$$\mathscr{K}_\mathbf{q} = \{\Delta\mathbf{v} \in \mathscr{X} : c(\Delta\mathbf{v},\mathbf{q}) \geq 0\}. \tag{3}$$

Basically, for a given realization of the uncertain parameter, such a set contains all the control vectors leading to no collision between the two objects. When $\mathbf{q}$ varies in $\mathscr{Q}$, (3) defines a family of feasibility sets. If these sets satisfy a convexity property, then there is a strong theoretical result on the solution of the scenario program, stated below.

Theorem 1 (Uncertain convex program [6] in three-dimension) *If $\mathscr{K}_\mathbf{q}$ is convex for all $\mathbf{q}$ in $\mathscr{Q}$ and if N is such that:*

$$(1-\varepsilon)^N + N\varepsilon(1-\varepsilon)^{N-1} + \frac{1}{2}(N-1)N\varepsilon^2(1-\varepsilon^{N-2}) \leq \beta, \tag{4}$$

*then there is a probability $1-\beta$, referred to as **the confidence level**, for the solution $\Delta\mathbf{v}^* = \Delta\mathbf{v}^*(\mathbf{q}^{(1)},\dots,\mathbf{q}^{(N)})$ of the scenario program* (2) *to satisfy:*

$$\mathbb{P}\{c(\Delta\mathbf{v}^*,\mathbf{q}) < 0\} \leq \varepsilon. \tag{5}$$

This theorem basically means that, under the convexity assumption for all the feasibility sets, there is a guarantee in probability for the solution of a sufficiently large scenario program to be admissible for the initial chance-constrained problem. However, even in this case, the provided solution will be sub-optimal since it is a global optimum for only a finite number of scenarios and there is no global optimal certificate for the genuine problem.
In the case when some feasibility sets $\mathscr{K}_{\mathbf{q}}$ for some $\mathbf{q}$ in $\mathscr{Q}$ are non convex sets, the solution of a scenario program may still be admissible for the original chance constrained problem, although the designer has no guarantee, even in a probabilistic sense. In addition, the obtained solution is in general a local optimum of the scenario program. In the present case of collision avoidance for rectilinear encounters, it turns out that the convexity property is not satisfied. As a result, even for large N, there is no guarantee that the solution of a scenario program will be admissible for the chance-constrained problem. Therefore, the validity of the solution would have to be checked *a posteriori* and its optimality can only be evaluated by comparing with alternative approaches when available.

5. COMPUTATION OF FUNCTION $c(\cdot,\mathbf{q})$ AND ITS GRADIENT

As mentioned in section 4., the scenario program (2) can be solved using state-of-the-art optimization solvers. To do so, one needs to evaluate the functions $c(\cdot,\mathbf{q}^{(j)})$ $(i=1,\dots,N)$ for any $\Delta\mathbf{v}\in\mathscr{X}$ and, to improve the efficiency of these solvers, their gradients if possible. Computing c requires to propagate the effects of a maneuver on the primary trajectory. In the sequel, it is assumed that they can be estimated with Keplerian dynamics.

5.1. The f and g Lagrange coefficients

The f and g functions first appear in the so-called Kepler problem [8, Chapter 2.11] which consists in propagating over time the position and velocity of a body on a Keplerian orbit. More precisely, if the position and velocity of an orbiting body are known at a given time t_1, its position and velocity can be found for any $t_2\leq t_1$ or any $t_2\geq t_1$, as linear combinations of the initial position and velocity vectors, whose coefficients are the f and g functions and their time derivatives $\dot{f}$ and $\dot{g}$. These four quantities are functions of time shift and initial conditions. Namely, for any (t_1,t_2):

$$\begin{aligned}\mathbf{r}^{t_2}&=f(\mathbf{r}^{t_1},\mathbf{v}^{t_1},t_2-t_1)\mathbf{r}^{t_1}+g(\mathbf{r}^{t_1},\mathbf{v}^{t_1},t_2-t_1)\mathbf{v}^{t_1},\\ \mathbf{v}^{t_2}&=\dot{f}(\mathbf{r}^{t_1},\mathbf{v}^{t_1},t_2-t_1)\mathbf{r}^{t_1}+\dot{g}(\mathbf{r}^{t_1},\mathbf{v}^{t_1},t_2-t_1)\mathbf{v}^{t_1}.\end{aligned}\tag{6}$$

The idea of introducing such functions comes from Kepler's laws, stating that a given orbit lies in a single plane. Using an angular parameter instead of t, analytic expressions for f and g and their time derivatives may be derived by solving the equations of motion in the two-body problem. The relationship between time and the orbital angle is given by the so-called Kepler equation. As a result, seen as functions of time, f, g, $\dot{f}$ and $\dot{g}$ are implicitly defined and can be computed by solving a transcendental equation. It is done here via a Newton-Raphson algorithm. See [3, Chapter 4] or [9, Chapter 8] for details.

5.2. Computing $c(\Delta\mathbf{v}, \mathbf{q})$

For any given scenario $\mathbf{q} \in \mathscr{Q}$, we now want to compute $c(\Delta\mathbf{v}, \mathbf{q})$ as a function of the impulse $\Delta\mathbf{v}$. Recall that, in the framework of rectilinear encounters between spherical objects, the collision set in the space of relative coordinates at $t = 0$ is an infinite right cylinder of revolution. Its axis contains the origin and is oriented along the relative velocity vector (see Figure 2). As a result, the condition for the occurrence of a collision can be expressed as a single inequality $c(\Delta\mathbf{v}, \mathbf{q}) < 0$. It basically states that the squared magnitude of the projection of the relative position vector onto the plane orthogonal to the relative velocity has to be smaller than the square of the combined radius. Let $\mathbf{r}_p^0(\Delta\mathbf{v}, \mathbf{q})$ and $\mathbf{v}_p^0(\Delta\mathbf{v}, \mathbf{q})$ be respectively the primary position and velocity at $t = 0$ after a maneuver $\Delta\mathbf{v}$ is performed at $t = \tau$. Function c writes as:

$$c(\Delta\mathbf{v}, \mathbf{q}) = \|\mathbf{r}_p^0(\Delta\mathbf{v}, \mathbf{q}) - \mathbf{r}_s^0\|^2 - \left((\mathbf{r}_p^0(\Delta\mathbf{v}, \mathbf{q}) - \mathbf{r}_s^0)^T \cdot \frac{\mathbf{v}_p^0(\Delta\mathbf{v}, \mathbf{q}) - \mathbf{v}_s^0}{\|\mathbf{v}_p^0(\Delta\mathbf{v}, \mathbf{q}) - \mathbf{v}_s^0\|} \right)^2 - R^2. \quad (7)$$

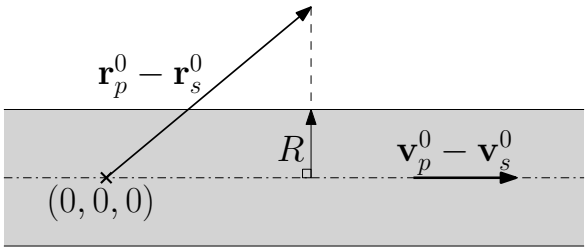

Figure 2: Tube of collision

In order to evaluate $c(\Delta\mathbf{v}, \mathbf{q})$, we now need to compute the primary position $\mathbf{r}_p^0(\Delta\mathbf{v}, \mathbf{q})$ and velocity $\mathbf{v}_p^0(\Delta\mathbf{v}, \mathbf{q})$. In the present study, as in [11], the effect of the maneuver $\Delta\mathbf{v}$ on the primary object is assumed to be computed under Keplerian dynamics, i.e. by neglecting the effects of orbital perturbations. Therefore, the Lagrange coefficients f and g can be used to evaluate $\mathbf{r}_p^0(\Delta\mathbf{v}, \mathbf{q})$ and $\mathbf{v}_p^0(\Delta\mathbf{v}, \mathbf{q})$.

Let us first propagate backwards the initial state $(\hat{\mathbf{r}}_p^0, \hat{\mathbf{v}}_p^0)$ to the instant τ of burn. According to formulas (6), the primary position and velocity just before the burn are given by:

$$\begin{aligned} \mathbf{r}_p^\tau(\mathbf{q}) &= f\left(\hat{\mathbf{r}}_p^0, \hat{\mathbf{v}}_p^0, \tau\right) \hat{\mathbf{r}}_p^0 + g\left(\hat{\mathbf{r}}_p^0, \hat{\mathbf{v}}_p^0, \tau\right) \hat{\mathbf{v}}_p^0, \\ \mathbf{v}_p^\tau(\mathbf{q}) &= \dot{f}\left(\hat{\mathbf{r}}_p^0, \hat{\mathbf{v}}_p^0, \tau\right) \hat{\mathbf{r}}_p^0 + \dot{g}\left(\hat{\mathbf{r}}_p^0, \hat{\mathbf{v}}_p^0, \tau\right) \hat{\mathbf{v}}_p^0. \end{aligned}$$

Note that all the previous quantities are independent of the control vector. The next step is to add the velocity increment $\Delta\mathbf{v}$ at $t = \tau$ and to finally propagate forwards the state to $t = 0$. The primary position and velocity vectors after the burn are then given by:

$$\mathbf{r}_p^0(\Delta\mathbf{v}, \mathbf{q}) = f\left(\mathbf{r}_p^\tau(\mathbf{q}), \mathbf{v}_p^\tau(\mathbf{q}) + \Delta\mathbf{v}, -\tau\right) \mathbf{r}_p^\tau(\mathbf{q}) + g\left(\mathbf{r}_p^\tau(\mathbf{q}), \mathbf{v}_p^\tau(\mathbf{q}) + \Delta\mathbf{v}, -\tau\right) \left(\mathbf{v}_p^\tau(\mathbf{q}) + \Delta\mathbf{v}\right), \quad (8)$$

$$\mathbf{v}_p^0(\Delta\mathbf{v}, \mathbf{q}) = \dot{f}\left(\mathbf{r}_p^\tau(\mathbf{q}), \mathbf{v}_p^\tau(\mathbf{q}) + \Delta\mathbf{v}, -\tau\right) \mathbf{r}_p^\tau(\mathbf{q}) + \dot{g}\left(\mathbf{r}_p^\tau(\mathbf{q}), \mathbf{v}_p^\tau(\mathbf{q}) + \Delta\mathbf{v}, -\tau\right) \left(\mathbf{v}_p^\tau(\mathbf{q}) + \Delta\mathbf{v}\right). \quad (9)$$

Plugging these expressions into (7) allows to evaluate $c(\Delta\mathbf{v}, \mathbf{q})$. As previously mentioned, the inequality $c(\cdot, \mathbf{q}) \geq 0$ does not satisfy any convexity property.

5.3. Computing $\partial_1 c(\Delta\mathbf{v}, \mathbf{q})$

In the present approach, the gradient of the function $c(\cdot, \mathbf{q})$ can be computed analytically, allowing us in part 6. to use more efficient optimization solver. This part is dedicated to the derivation of a formula for $\partial_1 c(\Delta\mathbf{v}, \mathbf{q})$, where ∂_1 denotes the partial derivatives of a function with respect to its first input.

From equations (8) and (9), it comes that:

$$\begin{aligned}
\partial_1 \mathbf{r}_p^0(\Delta\mathbf{v}, \mathbf{q}) &= \partial_2 f\left(\mathbf{r}_p^\tau, \mathbf{v}_p^\tau + \Delta\mathbf{v}, -\tau\right)\mathbf{r}_p^\tau + \partial_2 g\left(\mathbf{r}_p^\tau, \mathbf{v}_p^\tau + \Delta\mathbf{v}, -\tau\right)\mathbf{v}_p^\tau + g\left(\mathbf{r}_p^\tau, \mathbf{v}_p^\tau + \Delta\mathbf{v}, -\tau\right), \quad (10)\\
\partial_1 \mathbf{v}_p^0(\Delta\mathbf{v}, \mathbf{q}) &= \partial_2 \dot{f}\left(\mathbf{r}_p^\tau, \mathbf{v}_p^\tau + \Delta\mathbf{v}, -\tau\right)\mathbf{r}_p^\tau + \partial_2 \dot{g}\left(\mathbf{r}_p^\tau, \mathbf{v}_p^\tau + \Delta\mathbf{v}, -\tau\right)\mathbf{v}_p^\tau + \dot{g}\left(\mathbf{r}_p^\tau, \mathbf{v}_p^\tau + \Delta\mathbf{v}, -\tau\right), \quad (11)
\end{aligned}$$

where ∂_2 denotes the partial derivative with respect to the second variable of the considered function. Note that the partial derivatives of the f and g functions can be derived from their analytic expressions. Let us now define:

$$\mathbf{u}_r^0(\Delta\mathbf{v}, \mathbf{q}) = \frac{\mathbf{v}_p^0(\Delta\mathbf{v}, \mathbf{q}) - \mathbf{v}_s^0}{\|\mathbf{v}_p^0(\Delta\mathbf{v}, \mathbf{q}) - \mathbf{v}_s^0\|}, \quad (12)$$

and rewrite $c(\Delta\mathbf{v}, \mathbf{q})$ as:

$$c(\Delta\mathbf{v}, \mathbf{q}) = c'(\Delta\mathbf{v}, \mathbf{q}) - c''(\Delta\mathbf{v}, \mathbf{q})^2,$$

where the functions c', c'' are defined by:

$$\begin{aligned}
c'(\Delta\mathbf{v}, \mathbf{q}) &= \|\mathbf{r}_p^0(\Delta\mathbf{v}, \mathbf{q}) - \mathbf{r}_s^0\|^2 - R^2,\\
c''(\Delta\mathbf{v}, \mathbf{q}) &= \left(\mathbf{r}_p^0(\Delta\mathbf{v}, \mathbf{q}) - \mathbf{r}_s^0\right)^T \mathbf{u}_r^0(\Delta\mathbf{v}, \mathbf{q}).
\end{aligned}$$

The $c'(\cdot, \mathbf{q})$ function can be seen as a composite function, namely:

$$c'(\cdot, \mathbf{q}) : \Delta\mathbf{v} \mapsto \mathbf{r}_p^0(\Delta\mathbf{v}, \mathbf{q}) - \mathbf{r}_s^0 \mapsto \|\mathbf{r}_p^0(\Delta\mathbf{v}, \mathbf{q}) - \mathbf{r}_s^0\|^2,$$

whose gradient with respect to $\Delta\mathbf{v}$, is classically given by:

$$\partial_1 c'(\Delta\mathbf{v}, \mathbf{q}) = 2\partial_1 \mathbf{r}_p^0(\Delta\mathbf{v}, \mathbf{q})^T(\mathbf{r}_p^0(\Delta\mathbf{v}, \mathbf{q}) - \mathbf{r}_s^0).$$

Let us now focus on the computation of $\partial_1 c''(\Delta\mathbf{v}, \mathbf{q})$. The first step consists in computing the gradient of $c''(\cdot, \mathbf{q})$ as a function of $\partial_1 \mathbf{u}_r^0(\cdot, \mathbf{q})$. In what follows, the dependence in the impulse $\Delta\mathbf{v}$ will be omitted to lighten the notations. Here we get:

$$\partial_1 c''(\Delta\mathbf{v}, \mathbf{q}) = \partial_1 \mathbf{r}_p^{0T} \mathbf{u}_r^0 + \partial_1 \mathbf{u}_r^{0T}(\mathbf{r}_p^0 - \mathbf{r}_s^0).$$

The second step is to compute $\partial_1 \mathbf{u}_r^0(\Delta\mathbf{v}, \mathbf{q})$ and is more technical. The function $\mathbf{u}_r^0(\cdot, \mathbf{q})$ can be seen in its turn as a composite function, namely:

$$\begin{array}{rccccc}
\mathbf{u}_r^0(\cdot, \mathbf{q}) : \mathbb{R}^3 & \mapsto & \mathbb{R}^3 & \mapsto & \mathbb{R}^3 \\
\Delta\mathbf{v} & \mapsto & \mathbf{v}_p^0(\Delta\mathbf{v}, \mathbf{q}) - \mathbf{v}_s^0 & \mapsto & \psi(\mathbf{v}_p^0(\Delta\mathbf{v}, \mathbf{q}) - \mathbf{v}_s^0) = \frac{\mathbf{v}_p^0(\Delta\mathbf{v}, \mathbf{q}) - \mathbf{v}_s^0}{\|\mathbf{v}_p^0(\Delta\mathbf{v}, \mathbf{q}) - \mathbf{v}_s^0\|}.
\end{array}$$

Using the first order Taylor expansion of the function $\psi : \mathbb{R}^3 \mapsto \mathbb{R}^3, x \mapsto \frac{x}{\|x\|}$, the Jacobian matrix of ψ writes:

$$J_\psi(x) = \frac{1}{\|x\|}\left(I_3 - \frac{xx^T}{\|x\|^2}\right).$$

Hence:

$$\begin{aligned}
\partial_1 \mathbf{u}_r^0(\Delta\mathbf{v}, \mathbf{q}) &= J_\psi(\mathbf{v}_p^0 - \mathbf{v}_s^0)\partial_1 \mathbf{v}_p^0, \\
&= \left(I_3 - \frac{(\mathbf{v}_p^0 - \mathbf{v}_s^0)(\mathbf{v}_p^0 - \mathbf{v}_s^0)^T}{\|\mathbf{v}_p^0 - \mathbf{v}_s^0\|^2}\right)\frac{\partial_1 \mathbf{v}_p^0}{\|\mathbf{v}_p^0 - \mathbf{v}_s^0\|}, \\
&= \frac{1}{\|\mathbf{v}_p^0 - \mathbf{v}_s^0\|}\left(I_3 - \mathbf{u}_r^0 \mathbf{u}_r^{0T}\right)\partial_1 \mathbf{v}_p^0.
\end{aligned}$$

The gradient of $c''(\cdot, \mathbf{q})$ writes:

$$\partial_1 c''(\Delta\mathbf{v}, \mathbf{q}) = \partial_1 \mathbf{r}_p^{0T}\mathbf{u}_r^0 + \frac{\partial_1 \mathbf{v}_p^{0T}}{\|\mathbf{v}_p^0 - \mathbf{v}_s^0\|}\left(I_3 - \mathbf{u}_r^0 \mathbf{u}_r^{0T}\right)^T(\mathbf{r}_p^0 - \mathbf{r}_s^0).$$

Lastly, after some simplifications, the gradient of $c(\cdot, \mathbf{q})$, given by:

$$\partial_1 c(\Delta\mathbf{v}, \mathbf{q}) = \partial_1 c'(\Delta\mathbf{v}, \mathbf{q}) - 2c''(\Delta\mathbf{v}, \mathbf{q})\partial_1 c''(\Delta\mathbf{v}, \mathbf{q}),$$

equals:

$$\partial_1 c = 2\left(\partial_1 \mathbf{r}_p^0 - \frac{(\mathbf{r}_p^0 - \mathbf{r}_s^0)^T\mathbf{u}_r^0}{\|\mathbf{v}_p^0 - \mathbf{v}_s^0\|}\partial_1 \mathbf{v}_p^0\right)^T (I_3 - \mathbf{u}_r^0 \mathbf{u}_r^{0T})(\mathbf{r}_p^0 - \mathbf{r}_s^0). \tag{13}$$

6. NUMERICAL RESULTS

The scenario approach can deal with any given date of avoidance maneuver. However for the sake of comparison, we choose here a specific configuration for the burn, namely one half orbital period before conjunction. In the case of a circular orbit, a tangential maneuver is a classical choice to maximize the radial separation between the two objects [14]. Thus, the first example validates our method by comparing it to this heuristic. The second example is an encounter on an elliptical orbit, for which no intuitive solution exists, but that can still be tackled by the scenario approach. For both cases, the positions $\hat{\mathbf{r}}_p^0$ and $\mathbf{r}_s^0$ of each orbiting object, follow independent normal probability distribution laws while uncertainty on velocities is neglected: the variables $\hat{\mathbf{v}}_p^0$ and $\mathbf{v}_s^0$ are in fact deterministic. It is a usual assumption for short-term encounters [2]. Scenarios are then randomly sampled accordingly to these probability distribution laws.

Solutions will be expressed in the local orbital frame (x, y, z) depicted in Figure 3: it is attached to the primary orbit propagated backwards to $t = \tau$ from the mean position-velocity vector $\mathbb{E}(\hat{\mathbf{r}}_p^0, \hat{\mathbf{v}}_p^0)$. The x axis is along the orbital velocity, the z axis points opposite to the orbital momentum and the y axis completes the orthogonal frame.

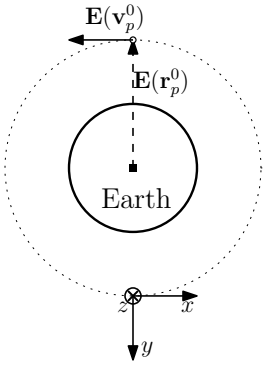

Figure 3: Configuration of the collision avoidance maneuver

Let us now describe the main steps of the search for optimality:

1. Generate N scenarios $\mathbf{q}^{(1)}, \ldots, \mathbf{q}^{(N)}$.
2. Solve the associated scenario program.
   (a) If there is no solution, then go back to step 1.
   (b) Otherwise let $\Delta\mathbf{v}$ be the obtained solution and go to step 3.
3. Compare the current cost $\|\Delta\mathbf{v}\|$ to the last memorized $\|\Delta\mathbf{v}^*\|$.
   (a) If $\|\Delta\mathbf{v}\| \leq \|\Delta\mathbf{v}^*\|$, go to step 4.
   (b) Otherwise go back to step 1.
4. Check the feasibility of the current $\Delta\mathbf{v}$ for the original chance constrained problem via a Monte Carlo method.
   (a) If $\mathbb{P}\{c(\Delta\mathbf{v}, \mathbf{q}) < 0\} \leq \varepsilon$, then $\Delta\mathbf{v}^* \leftarrow \Delta\mathbf{v}$ and go back to step 1.
   (b) Otherwise go back to step 1.

This iterative algorithm basically solves scenario programs and only keeps solutions admissible to the chance-constrained problem and improving the cost. The loop stops when the maximum number of iterations has been reached. The user can possibly change the value of N to extend the search. In this study, $N = 1,000$ and scenario programs are solved with fmincon in ©Matlab 2014a.

As a reference for comparison, a simple homemade line search method is used, providing Solutions labeled 0. More precisely, solutions are obtained by a dichotomous search along a direction fixed *a priori*. Similarly to what is proposed in [14], it is chosen along the x axis. The dichotomous search stops when the risk lies in $[0.99\varepsilon, \varepsilon]$, according to Monte Carlo trials.

6.1. Example 1

This first example is a real conjunction alert sent by the JSpOC to our industrial partner Airbus Defence and Space. The primary orbit is circular and the risk without mitigation is 1.9×10^{-3}.

A summary of the different computed solutions is given in Table 1. It is noticeable that the two solutions coming from the two different approach are almost equal, confirming the heuristic choice of Solution 0. Figure 4 depicts the histogram of logarithmic normalized miss distances ($\log_{10}\sqrt{1+c/R^2}$) for a random sampling of 10^4 relative trajectories. The distribution resulting from the maneuver shows no collision (negative values), unlike the uncontrolled case.

No.	$\Delta\mathbf{v}_x$ (mm/s)	$\Delta\mathbf{v}_y$ (mm/s)	$\Delta\mathbf{v}_z$ (mm/s)	$\|\Delta\mathbf{v}\|$ (mm/s)	$\mathbb{P}\{c(\Delta\mathbf{v},\mathbf{q})<0\}$
0	-22.510	0	0	22.510	1.0×10^{-4}
1	-22.495	0.625	0.003	22.504	9.7×10^{-5}

Table 1: Solutions

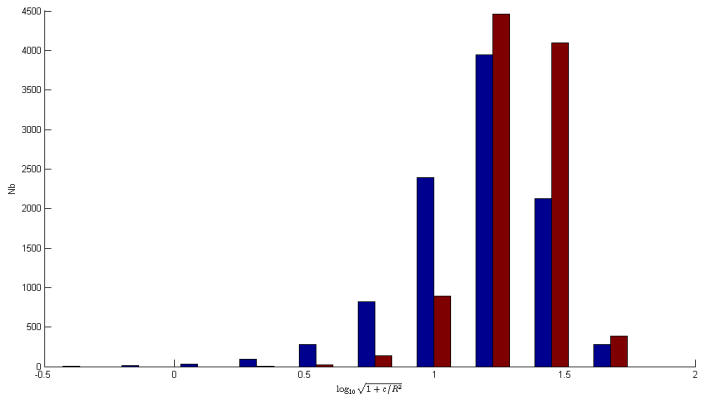

Figure 4: Histogram of miss distances: without mitigation (blue) and with maneuver (red)

6.2. Example 2

The primary orbit is non-circular with an eccentricity of 0.741. Input data are obtained by modifying case number 9 in [1] in order to obtain a short-term encounter. Mean values are given in Table 2 and covariance matrices in equation (14) for the primary (left side) and for the secondary (right side):

$$\begin{pmatrix} 67.0143 & 14.5722 & 31.3632 \\ * & 3.2133 & 6.8234 \\ * & * & 14.7289 \end{pmatrix}, \begin{pmatrix} 67.0146 & 14.5721 & 31.3630 \\ * & 3.2133 & 6.8234 \\ * & * & 14.7288 \end{pmatrix}. \tag{14}$$

Object	Primary	Secondary
Position (km)	$[-5532.700\ 20132.674\ 40010.549]$	$[-5532.694\ 20132.677\ 40010.554]$
Velocity (km/s)	$[-1.450945\ -0.311609\ -0.671302]$	$[-1.450947\ -0.311608\ 0.671301]$

Table 2: Mean values for object's position and velocity

Collision probability without any maneuver is 3.24×10^{-1}. As shown in Table 3, Solution 0 is 16.7% more costly than the one obtained via the scenario approach. It can be explained by the fact that, for a non-circular orbit, a tangential maneuver does not demonstrate any specific advantage. This shows the usefulness of the scenario approach that can handle configurations for which it is hard to heuristically derive fuel-efficient maneuvers. The histogram of logarithmic normalized miss distances is depicted in Figure 5 and illustrates the safety introduced by the control law.

No.	$\Delta\mathbf{v}_x$ (mm/s)	$\Delta\mathbf{v}_y$ (mm/s)	$\Delta\mathbf{v}_z$ (mm/s)	$\|\Delta\mathbf{v}\|$ (mm/s)	$\mathbb{P}\{c(\Delta\mathbf{v},\mathbf{q})<0\}$
0	-0.3315	0	0	0.3315	1.0×10^{-4}
1	-0.2430	0.0094	-0.1469	0.2841	8.0×10^{-5}

Table 3: Solutions

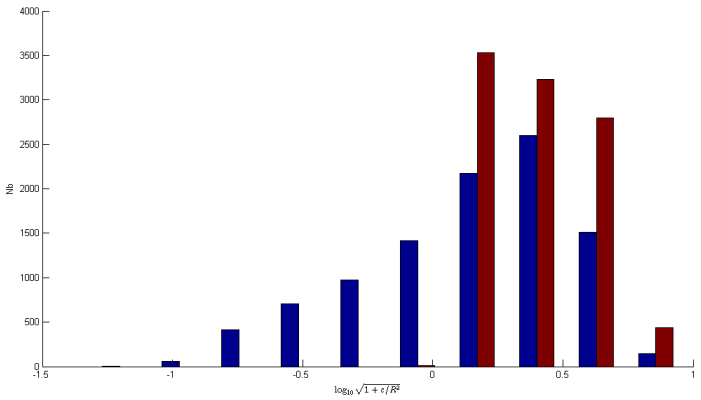

Figure 5: Histogram of miss distances: without mitigation (blue) and with maneuver (red)

7. CONCLUSION

A method to design collision avoidance maneuvers for rectilinear space encounters has been proposed. Based on the scenario approach for chance-constrained optimization, it provides the user with admissible solutions and has several advantages. First of all, unlike some other works in the literature, it does not reduce the original dimension of the optimization space for the impulse. As a result, it does not require any heuristic knowledge on the optimal solution. Secondly, the f and g functions prove to be a convenient way to analytically compute the constraints and their gradient with respect to the control vector in the scenario program. Additionally, this approach does not require any assumption on the nature of the uncertainty affecting the position and velocity of both objects, allowing for non-Gaussian probability distribution laws. Although this paper focuses on spherical objects, the method could be extended to other geometrical shapes such as polyhedrons, with applications to the International Space Station for instance. The only requirement ist to be able to derive the expression and compute the value of the collision equations as functions of both control vector and uncertain parameter.

ACKNOWLEDGMENT

The authors would like to thank Alexandre Falcoz from Airbus Defence and Space for the grant that partly supports this work.

8. References

[1] S. Alfano. Satellite conjunction monte carlo analysis. In Proceedings of AAS/AIAA Spaceflight Mechanics Meeting, number AAS 09-233, Savannah, Georgia, USA, February 2009.

[2] K.T. Alfriend, M.R. Akella, J. Frisbee, F.L. Foster, D-J Lee, and M. Wilkins. Probability of collision error analysis. Journal of Space Debris, 1(1):21–35, 1999.

[3] R.R. Bate, D.D. Mueller, and J.E. White. Fundamentals of Astrodynamics. Dover. Cambridge University Press, New York, USA, 1971.

[4] L. Blackmore and M. Ono. Convex chance constrained predictive control without sampling. In AIAA Guidance, Navigation, and Control Conference, pages 7–21, Chicago, Illinois, USA, 2009.

[5] G. Calafiore and M.C. Campi. Uncertain convex programs: randomized solutions and confidence levels. Mathematical Programming, 102(1):25–46, 2005.

[6] M.C. Campi and S. Garatti. The exact feasibility of randomized solutions of uncertain convex programs. SIAM Journal on Optimization, 19(3):1211–1230, 2008.

[7] F.K. Chan. Spacecraft Collision Probability. Aerospace Press, New York, USA, 2008.

[8] H.D. Curtis. Orbital Mechanics for Engineering Students. Dover. Butterworth-Heinemann, Oxford, UK, 2005.

[9] J.L. Junkins and H. Schaub. Analytic Mechanics of Space Systems. AIAA Education Series. AIAA, Reston, Virginia, USA, 2003.

[10] J.B. Mueller and R. Larsson. Collision avoidance maneuver planning with robust optimization. In 7th International ESA Conference on Guidance, Navigation and Control Systems, Tralee, County Kerry, Ireland, 2008.

[11] R.P. Patera and G.E. Peterson. Space vehicle maneuver method to lower collision risk to an acceptable level. Journal of Guidance, Control and Dynamics, 26(2):233–237, 2003.

[12] A. Prépoka. Stochastic programming. Kluwer Academic Publishers, Dordrecht, The Netherlands, 1995.

[13] I Ross. Modern Astrodynamics, chapter 6 Space trajectory optimization and L^1-optimal control problems. Elsevier Astrodynamics Series. Gurfil, P., 2007.

[14] N. Sánchez-Ortiz, M. Belló-Mora, and H. Klinkrad. Collision avoidance manoeuvres during spacecraft mission lifetime: Risk reduction and required δv. Advances in Space Research, 38(9):2107–2116, 2008.

[15] A. Shapiro, D. Dentcheva, and A. Ruszcyński. Stochastic Programming: Modeling and Theory. MPS-SIAM series on Optimization. SIAM, 2009.

[16] G.L. Slater, S.M. Byram, and T.W. Williams. Collision avoidance for satellites in formation flight. Journal of Guidance, Control and Dynamics, 29(5):1140–1146, 2006.

[17] D. A. Vallado. Fundamentals of Astrodynamics and Applications. Kluwer Academic Publishers, Dordrecht, The Netherlands, 2001.